

FIVE YEARS OF PROJECT META: AN ALL-SKY NARROW-BAND RADIO SEARCH FOR EXTRATERRESTRIAL SIGNALS

PAUL HOROWITZ

Lyman Laboratory of Physics, Harvard University, Cambridge, MA 02138

AND

CARL SAGAN

Center for Radiophysics and Space Research, Cornell University, Ithaca, NY 14853;
 and The Planetary Society, Pasadena, CA 91106

Received 1992 October 2; accepted 1993 March 30

ABSTRACT

We have conducted a 5 year search of the northern sky ($-30^\circ \leq \delta \leq 60^\circ$) for narrow-band radio signals near the 1420 MHz line of neutral hydrogen, and its second harmonic, using an 8.4×10^6 channel Fourier spectrometer of 0.05 Hz resolution and 400 kHz instantaneous bandwidth. The observing frequency was corrected both for motions with respect to three astronomical inertial frames, and for the effect of Earth's rotation, which provides a characteristic changing Doppler signature for narrow-band signals of extraterrestrial origin. Among the 6×10^{13} spectral channels searched, we have found 37 candidate events exceeding the average detection threshold of 1.7×10^{-23} W m $^{-2}$, none of which has been detected upon reobservation. The strongest of these appear to be dominated by rare processor errors. However, the strongest signals that survive culling for terrestrial interference lie in or near the Galactic plane. We describe the search and candidate events, and set limits on the prevalence of supercivilizations transmitting Doppler-precompensated beacons at H I or its second harmonic. We conclude with recommendations for future searches, based upon these findings, and a description of our next-generation search system.

Subject headings: extraterrestrial intelligence — radio lines: general

1. INTRODUCTION

More than 30 years ago, advances in radioastronomy made possible the first radio search for extraterrestrial intelligence (SETI), with the 1420 MHz hyperfine line of neutral atomic hydrogen suggested as a preferred (or “magic”) transmission frequency (Cocconi & Morrison 1959; Drake 1960). Of a wide range of speculative estimates of the abundance of advanced transmitting civilizations, some suggest large numbers ($\sim 10^6$) in the Milky Way (Shklovskii & Sagan 1966, especially chap. 29; Sagan 1973, especially pp. 164–179) (in which case, if civilizations are uniformly distributed through the Galactic plane, the nearest is ≈ 100 pc distant), while others propose that we are alone (Hart 1975; Tipler 1980). A scientific consensus seems to be that such searches are worth performing (Sagan et al. 1982), and some 60 observing programs have been undertaken to date (Tarter 1933)—but very few for more than a few hours at high (< 1 Hz) spectral resolution.

For the past 6 years we have been conducting Project META (Megachannel ExtraTerrestrial Assay), a continuous meridian transit search of the northern sky ($\delta = -30^\circ$ to $+60^\circ$) with an 8.4 million-channel spectrum analyzer connected to the Harvard/Smithsonian 26 m radiotelescope at Agassiz Station (Horowitz et al. 1986; Horowitz 1987; Horowitz & Clubok 1991). Successive 400 kHz spectra, at 0.05 Hz resolution, are examined for features characteristic of an intentional narrow-band beacon transmission. These spectra are centered most often on the 1420 MHz (21 cm) line, or its second harmonic (2840 MHz), referenced successively to the local standard of rest (LSR), the Galactic barycenter (GBC), and the cosmic microwave background rest frame (CMB). At such high spectral resolution, the accelerating frame of the rotating and orbiting Earth introduces a significant and char-

acteristic Doppler “chirp” for extraterrestrial but not for terrestrial signals, which is compensated by a precisely swept (“agile”) receiver. The 0.5 half-power beam width (at $\lambda = 21$ cm) dwells a minimum of 2 minutes on each potential source position in the sky, allowing time for six integrations (two polarizations, three inertial frames) of 20 s each.

Since META began (in late 1985) we have covered the sky 3 times at $\lambda = 21$ cm and nearly twice at $\lambda = 10.5$ cm. In that time, there have been numerous extrastatistical spectral features, of which 37 have the characteristic signature of a narrow-band carrier in an inertial frame. However, in spite of reobservations over a range of time scales, none of these “signals” has been detected a second time.¹ In this paper we describe the nature of these transient events and our reasons for believing that they cannot be identified as signals of extraterrestrial origin; we then describe the consequent limits on the prevalence of transmitting civilizations, assuming that we have a null detection. We conclude with some recommendations for future searches, and a description of our planned follow-on search system.

2. THE META SYSTEM

The META system has been described in detail elsewhere (Horowitz et al. 1986); we provide only a brief summary here. The antenna's beam (0.5 at $\lambda = 21$ cm, 0.25 at $\lambda = 10.5$ cm; hereafter we give parameters for $\lambda = 21$ cm only) performs a transit search of the sky, being moved in declination by one half-power beamwidth every day (or every 2 days), to cover the

¹ We use *observation* to mean the routine collection of spectral data (whatever its character), reserving the word *detection* for observations displaying excess narrow-band power.

sky from $\delta = -30^\circ$ to $\delta = +60^\circ$ in a period of 200–400 days. A pair of low-noise GaAsFET amplifiers (one for each polarization) and a downconverter/IF system with agile heterodyne oscillators (to cancel the Doppler chirp caused by Earth's rotation) feed the digital spectrum analyzer, constructed as an array of 128 (+16 redundant) parallel processors, each with a Motorola 68000 microprocessor, coprocessor, RAM, etc., to perform an 8.4×10^6 channel complex Fourier transform from the 7 bit digitized quadrature baseband voltages. Its channels are $B = 0.05$ Hz wide, resulting in an overall instantaneous bandwidth of 400 kHz. These narrow channels were chosen to match the natural bandwidth of carriers propagated through the interstellar medium (Cordes & Lazio 1991), for optimum detection of interstellar carriers. META is relatively insensitive to other kinds of signals, e.g., pulses or rapidly swept carriers. As justification for a "carrier only" search, one might plausibly expect a diversity of beacon protocols (including both carriers and pulses), corresponding to an expectation that different emerging civilizations will adopt different search strategies. Note, in this context, that META would detect a signal that includes a strong and unchanging (or slowly changing) narrow-band spectral feature, whether or not it includes other information-bearing components; it is in this sense that we use the term *carrier* in this paper.

META's bandwidth examines the close neighborhood of a particular chosen frequency. Its instantaneous bandwidth brackets reasonable uncertainties in calculated Doppler shift for a given choice of inertial frame ($\pm 40 \text{ km s}^{-1}$ at 1420 MHz), but is not sufficient to cover all three chosen frames simultaneously (their velocities differ by 600 km s^{-1} , or 3 MHz at 1420

MHz). Thus the system alternates observations among the three frames and two polarizations, finishing one complete cycle in the time it takes a point source to drift through the beam. Given the absence of known narrow-band microwave sources of astrophysical origin, we carried out extensive tests of system performance. In particular, the antenna beamwidth and system sensitivity were verified by drift scans of known continuum sources; the real-time Doppler predictions were compared with independent calculations done at Arecibo Observatory; and a suite of fixed and drifting carriers were injected at baseband, IF, and microwave frequencies, to verify correct operation of the chirped spectrometer system.

Figure 1 shows the META system, and Table 1 summarizes its observing parameters. On-line software computes ephemeris information and controls the local oscillators (LO), (1) setting the first LO and the polarization switch at the beginning of each 20 s integration interval τ_i ($B\tau_i = 1$) such that the center of the received band corresponds to the chosen frequency as observed in the chosen reference frame, and (2) sweeping the second LO to compensate for the Doppler chirp caused predominantly by Earth's rotation. The control computer also (3) orchestrates overall timing (frame buffering and initiation of Fourier transforms), (4) checks for processor errors by using 16 redundant processors (1 million channels), (5) examines the 8.4 million-channel spectra for unusual signal features, and (6) archives numerical and graphical information connected with unusual signals or system malfunction.

These last two processes are of particular interest here. Each Fourier processor computes 2^{16} (64 K) complex channels of the full 2^{23} channel transform; the individual processors then compute the power spectrum (square modulus) and perform

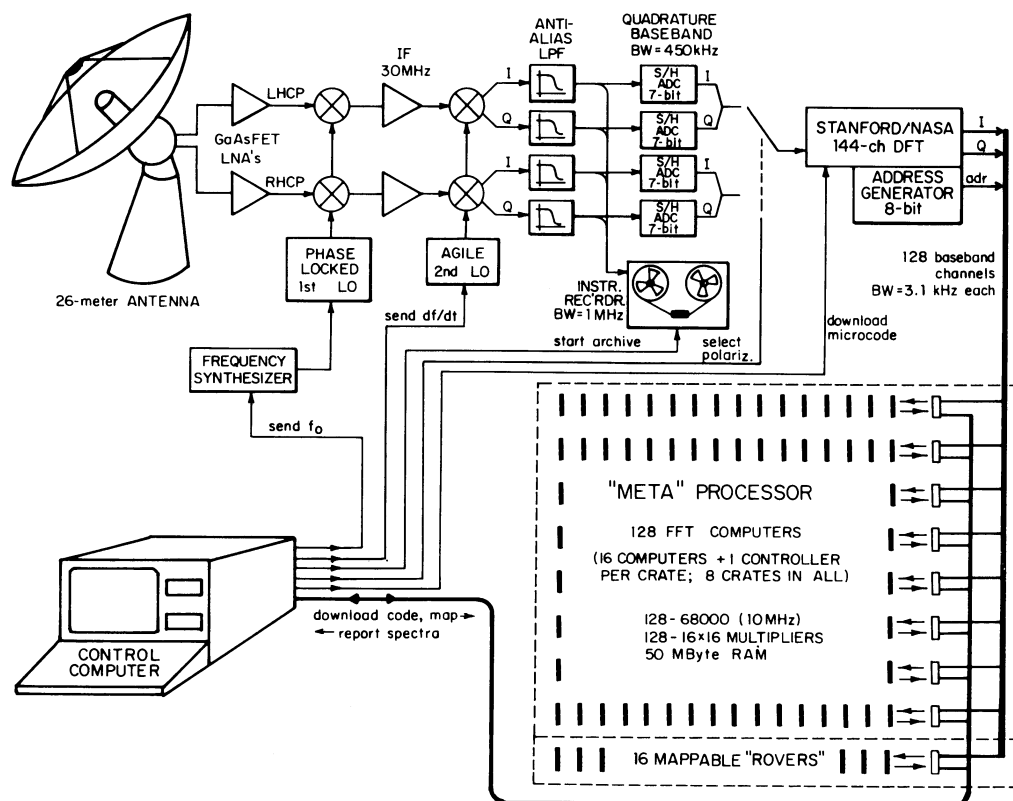


FIG. 1.—Block diagram of the META project: high-resolution megachannel SETI at the Harvard/Smithsonian 26 m radiotelescope

TABLE 1
PROJECT META PARAMETERS

ANTENNA
26-meter equatorial Cassegrain
FEEDS
21-cm and 10-cm dual-polarization (circular or linear)
AMPLIFIERS
1.4–1.7 GHz and 2.8 GHz GaAsFET; $T_r = 50\text{K}$
SPECTROMETER
8,388,608 channels
0.05 Hz per channel (400 kHz total bandwidth)
20-second integrations ($B\tau = 1$), chirped LO
continual self-test via redundant processors
SKY COVERAGE
declination -30° to $+60^\circ$ (68% of sky)
0.5° per day, 210 days per frequency choice
FREQUENCIES
H_i , $2 \times H_i$
corrected to
heliocenter/LSR
galactic barycenter
cosmic microwave background
frequencies and polarizations alternated on successive integrations
SENSITIVITY
$T_r \approx 85\text{K}$; total power receiver ($K_S = 1$)
$0.7\text{--}13 \times 10^{-23} \text{ W/m}^2$ for $30P_0$ detection of celestial carrier
in bandpass; average sensitivity $= 1.7 \times 10^{-23} \text{ W/m}^2$
ARCHIVING
summary data for integrations with peak above $20P_0$
baseline and “context” graphs for integrations with peak above $20.8P_0$
eight integrations following a trigger are also archived

Meta-system-v2.3
gmt 22:36 :00 26 Nov-1986
sdtime: 22:12:00 declin: 0.000000
144 good procs: 128 data and 16 rovers

run #4 started: 22:35:82 hits:4231
rest frame: b> Heliocenter/LSR
 $f = 1420.40575\text{MHz}$ $v = 10.00 \text{ km/s}$
RA: 18.0000 hrs decl: 30.0000 deg
polarization: Left

biggest peaks:
57.68 sig @ 28.75190 kHz
56.34 sig @ 28.75075 kHz
55.41 sig @ 28.75037 kHz
54.59 sig @ 28.75195 kHz
54.37 sig @ 28.75199 kHz
54.15 sig @ 28.75028 kHz
53.82 sig @ 28.75090 kHz

daily high:
72.42 sig @ 28.75037 kHz (d)

Possible signal of extraterrestrial origin
Notify operator immediately (run:4)
Possible signal of extraterrestrial origin

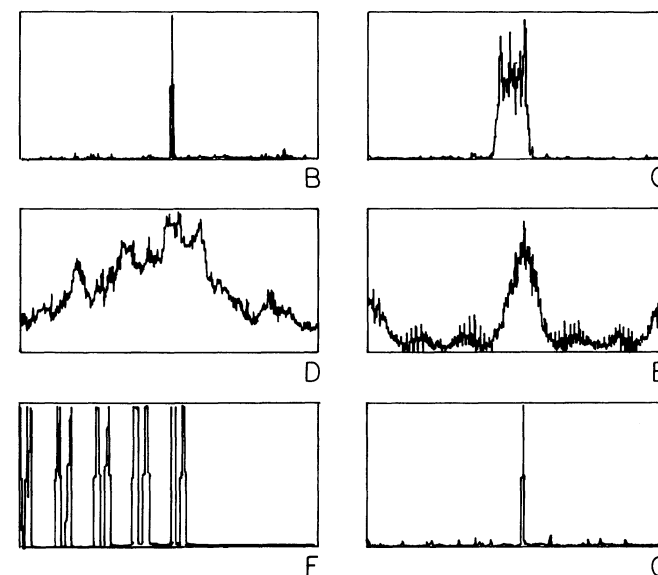
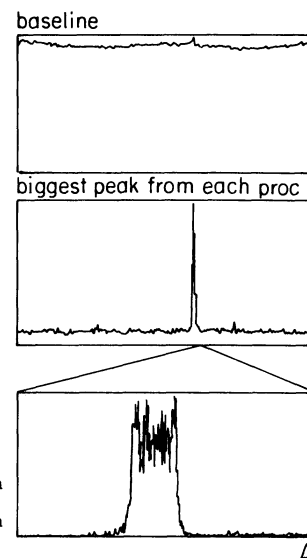


FIG. 2.—Examples of signals seen by META (*see text*). The peaks in B, G, and A (middle plot) are unresolved; their apparent width is a plotting artifact.

baseline subtraction and peak searching and sorting. Peaks that exceed the baseline by a preset threshold are reported to the central computer, where they are presented (Fig. 2). If the largest such peak exceeds a second “archiving” threshold, the screen display is written to disk and preserved permanently. This includes ephemeris information, a numerical summary of the largest peaks, and graphs showing both the immediate spectral region ($\pm 6 \text{ Hz}$ at the highest resolution: 0.05 Hz) and the full bandwidth ($\pm 200 \text{ kHz}$ at low resolution: 3 kHz).

When META detects a large peak (i.e., one that triggers archiving), it takes two further actions. First, it abandons the predetermined schedule of reference frame and polarization alternation, instead confining the next eight observations to the reference frame in which the suspicious event occurred; the largest spectral features from these integrations are archived, whether or not they exceed the normal threshold.² Second, it assigns a redundant processor to check the one reporting a large peak. Because of the delay caused by data pipelining through the system, such “immediate” reobservation is actually initiated 40 s later, separated by two observations in unrelated reference frames.

During our observations the thresholds have been set to produce a manageable amount of archived data, typically triggering archiving of ≈ 100 events per day. These cluster near the threshold, in a reasonably accurate approximation of the expected exponential distribution, with a few peaks per month

² Thus the weakest events reported are ~ 15 times the mean power per bin, P_0 (see § 3). During the eight follow-on observations the LO continues to step, so a persistent stable signal could produce detected frequencies that successively step through as much as 4% of the spectrometer bandwidth.

that depart significantly from this “noise tail.” It is these large peaks that we consider in detail in the rest of this paper. META, then, is designed to detect strong narrow-band signals near a chosen frequency, precompensated in one of three important inertial rest frames. The signal’s extraterrestrial origin is indicated by two characteristics: (1) it must display a Doppler chirp, precisely predictable given the epoch and celestial coordinate of the observation, and (2) it must display a sidereal motion, in particular that of a point-like source at fixed celestial coordinates. Thus terrestrial transmitters, or transmissions from orbiting satellites, should be effectively discriminated from true celestial sources; the former display no chirp and no motion (or, if mobile, Doppler shifts and motions unrelated to sidereal rotation), while the latter (except for geosynchronous satellites) generally display very large chirp rates, as well as rapid motions in sidereal coordinates.

META's sensitivity, listed in Tables 1 and 3, is not completely uniform: maximum sensitivity ($7 \times 10^{-24} \text{ W m}^{-2}$) is achieved only for sources that are observed on the beam axis and centered in a spectral frequency bin. Because the antenna declination is incremented each day by the half-power beamwidth, the sensitivity for sources halfway between telescope declinations is reduced by a factor of 2, with a similar maximum loss for sources observed at the half-power points in hour angle. Combined with this spatial nonuniformity is a variation of sensitivity in the spectral domain, known as "scalloping," whereby the full sensitivity (achieved for a signal whose frequency is centered on a spectral bin) is degraded by as much as 3.9 dB if the signal's frequency lies halfway between bins. These effects combine to produce a sensitivity that ranges from $0.7\text{--}13 \times 10^{-23} \text{ W m}^{-2}$, with a mean sensitivity of $1.7 \times 10^{-23} \text{ W m}^{-2}$.

3. META CANDIDATE SIGNALS

The archived peaks mainly fall into a few distinctive categories, most of which are shown in Figure 2. The top portion (labeled A) shows the archived screen display, a snapshot of the full META screen as it appears during normal operation; it is redrawn every 20 s, the integration time for each 8.4 million-channel spectrum. The display shows the target coordinates, time and date, and reference frame (in this case the LSR). It also lists the run's seven largest peaks by intensity (power per channel) and frequency. The three graphs at the right are various views of the spectrum: The top graph shows the full megachannel spectrum, compressed to low resolution by averaging adjacent blocks of 64 K channels to form each displayed point (whose channel width is thus 3.125 kHz). The middle graph is similar, but with the *highest* point of each 64 K channel block displayed. The bottom graph is a high-resolution blowup of the 128 channels centered on the largest peak of the full 8.4 million-channel spectrum; individual points here correspond to frequencies separated by 0.05 Hz, $\sim 3 \times 10^{-11}$ of the observing frequency.

For the screen shown we have intentionally introduced a fixed-frequency interfering signal. It shows weakly in the top graph (which is what a 128 channel receiver would see), but quite strongly in the middle graph. The most information comes from the high-resolution graph at the bottom, where the signal's spectrum is seen to be broadened, with a flat-topped shape. This is characteristic of a fixed-frequency terrestrial signal, smeared out by the deliberate chirp of the receiver's LO as it looks for a similarly chirping celestial signal [whose observed chirp rate is dominated by the effect of Earth's rotation, given by $df/dt = -(f_0 \Omega^2 R_e / c) \cos \delta \cos \phi$ for a source of frequency f_0 at declination δ , observed at transit from a site at geographic latitude ϕ ; Ω is Earth's angular velocity, and c is the speed of light. For a source overhead at the equator the chirp is $df/dt = -0.16 \text{ Hz s}^{-1}$ for $f_0 = 1420 \text{ MHz}$; at our Agassiz Station site in Harvard, Massachusetts, the corresponding figure for a transiting source at $\delta = 0^\circ$ is $df/dt = -0.12 \text{ Hz s}^{-1}$].

The remaining examples—graphs B through G—show the bottom (high-resolution) graph for the most common categories of signal we have seen. In graph B we have introduced an artificial signal, correctly chirped to mimic a celestial source of fixed frequency. It is nicely collected into one channel, thanks to the receiver's corresponding antichirp. In this example it has ~ 50 times the intensity of the average channel fluctuation, and would not be mistaken for noise. However,

except for intensity it looks similar to the most common candidate signal—an isolated peak sufficiently large to attract attention, but whose intensity is in fact predicted to occur roughly once per day. These lie on the tail of the probability distribution for spectral power, which can be shown to be precisely exponential if the Fourier *amplitudes* (real and imaginary parts) are normally distributed with zero mean, as they will be for the Discrete Fourier Transform of a noiselike input time series (Groth 1975). In particular, the normalized probability density of the power P in a frequency bin is $p(P) = (1/P_0) \exp(-P/P_0)$, where P_0 is the mean power per bin; the probability of the power in a bin exceeding a threshold T times the mean is $\text{Probability}(P > TP_0) = \exp(-T)$. Thus for our daily harvest of $N = 3.3 \times 10^{10}$ independent frequency channels, the power in the largest will typically be $T = \ln N = 24$ times the mean power.

Noise-tail events dominate the archive; on a typical day the archive contains *only* noise-tail peaks (or, more precisely, it contains no peaks stronger than the statistically expected maximum of $\approx 24P_0$). In this paper, our interest centers on those unusual peaks that clearly exceed this level, which occur roughly once per week.

Graphs C–G in Figure 2 are from real data taken during 1986–1990 and illustrate the remaining classes of common candidate signal. In all cases the signals are much stronger than the noise tail, and have characteristic shapes as well. One finds a class of flat-topped peaks, as in graph C, the signature of a fixed-frequency carrier; graphs like this occur perhaps once per week. The reduced width (compared with A) is due to the factor of $\cos \delta$ for sources at declination δ (graph A was made with chirp appropriate to $\delta = 0$). The signal seen in graph D is the erratic behavior of a less stable transmitter with a stability of "only" 1 part in 100 million; these occur sporadically, perhaps averaging 1 or 2 events per week. In graph E we see the distinctive symmetrical pattern of a modulated carrier, its sidebands extending beyond the $\pm 6 \text{ Hz}$ of the displayed spectral region; these signals are rarer, occurring perhaps once per month.

The 1420–1427 MHz band, although "protected" by international agreement, is not without interference, particularly when scrutinized with sensitive receiving systems of high spectral resolution. Although transmissions in this band *are* prohibited (the band being designated exclusively for passive radioastronomy), the statutory limits on spurious emissions from legal transmissions at other frequencies permit devastating amounts of signal energy to be radiated at 1420 MHz. For example, it is a straightforward exercise to calculate that a 100 W transmitter at 710 MHz (in the UHF television band), with 60 dB suppression of harmonic power, located 100 km from our site, with isotropic antenna gain at both transmitter and receiver (typical of sidelobes), would deliver a signal strength $\sim 4 \times 10^4$ times the average channel noise power in our receiver. Given that there are many transmitters located within this distance, most operating at considerably greater power levels, it should not be surprising that we do indeed detect coherent signals, displaying a variety of modulation schemes, in the normal operation of our search program. Indeed, one might well wonder why we are not overwhelmed by such interference. It is difficult to estimate a priori the prevalence of such interfering out-of-band signals. Our relatively low rate probably results from the combined effects of the chirped receiver strategy (which spreads the signal power over many frequency channels, thus greatly reducing its peak value) and the shadow-

ing effect of intervening hilly terrain (which greatly limits the geographical area with line-of-sight propagation paths to the observatory).

In Figure 2, the pattern in F resulted from a processor failure, repeated during several integrations before it was automatically identified and replaced by the fault-tolerant redundant hardware. The META system has been remarkably free of failure, with only two faulty ICs (out of 20,000 total) during its 6 years of continuous operation; consequently we have seen few such events. In G we show a plot displayed at 17:57 UT on 1986 October 10, just the sort of signal we might expect from an extraterrestrial source. It is an unresolved carrier (like the test signal in B), apparently of fixed frequency in celestial coordinates (a property exhibited only by the signals in B, E, and G). It is far above the noise tail ($66P_0$). But it has never repeated during reobservations of those sky coordinates. Perhaps more significant, the signal did not repeat even during any of the adjacent 20 s integrations.

Not shown in Figure 2, but relatively common nonetheless, are broadened features whose overall spectral envelopes are closer to Gaussian or Lorentzian than are the flat-topped shapes of A and C. Although they do not fit the model of a minimum bandwidth carrier, such signals obviously should not be eliminated from further consideration: They could arise, for example, from a beacon whose transmission frequency is not swept so as to cancel the Doppler effects of a rotating planet; from a distant carrier passing through a large column density of Galactic plasma (Cordes & Lazio 1991); from a relatively short pulse (or train of pulses) of pulse width ≈ 1 s; or from a slowly modulated carrier, with information bandwidth ≈ 1 Hz. In subsequent scattergrams we have retained these broadened peaks, grouped into categories according to their widths.

3.1. Reobservations

The celestial coordinates of candidate signals are observed more than once. Reobservations occur in three ways: (1) As described above, META's real-time algorithms force a return to the reference frame and polarization in which a large peak is seen, beginning ~ 40 s after the initial detection, and continuing for ~ 3 minutes (after which time the source will have drifted out of the antenna's beam); (2) The antenna's declination is often left unchanged for a second day (noted in Table 2), if the operator notes a suspicious event; and (3) manual reobservations in sidereal tracking mode are made for the most interesting candidate signals found by META. In the latter observations, which are typically carried out annually, the antenna follows the recorded sky coordinate of each interesting signal for at least 100 integrations (30 minutes).

4. RESULTS

Figures 3a–3c show the declination coverage versus Julian date of the bulk of META's observations. We have grouped the data into three runs according to frequency: runs A and C are at 1420 MHz, and run B is at the second harmonic, 2840 MHz. In this analysis we have omitted the initial year of operation (which includes the event shown in Fig. 2, graph G), because ongoing improvements during that period rendered the data nonuniform in sensitivity. In run A the set of points at low declination are at $\delta = -45^\circ$, the "parking" position for the telescope (for snowstorms, etc.), during which we continued to take data; in subsequent runs we decided that the elevated noise temperature and increased interference close to the

TABLE 2
EVENTS PLOTTED IN FIGURES 5B–7B

RA ^a	DEC ^a	Peak ^b	Freq ^c	Frame-Pol ^d	Type ^e	Date ^f	UT
RUN A: 1420 MHz							
00.87	57.5	28.0	-61.6	GBC-H	1	6942+	13:24
06.08	-3.5	29.8	-24.2	CMB-H	1	6782	05:09
06.23	9.5	28.0	-41.1	GBC-V	1	6822	02:41
11.58	31.5	28.2	-197.8	GBC-V	1	6876	04:29
21.15	-21.0	29.0	53.0	LSR-V	1	6737	23:08
21.98	38.5	33.6	170.7	CMB-H	4	6894	13:41
RUN B: 2840 MHz							
00.82	3.25	29.4	91.9	CMB-H	1	7735+	09:15
01.30	-22.00	28.8	64.0	CMB-V	1	7577+	20:06
01.83	7.00	28.2	-189.9	GBC-H	1	7769	08:03
05.73	6.00	29.2	-184.0	GBC-H	1	7326	17:02
08.00	-8.50	746.6	58.7	LSR-V	1	7415+	13:27
08.03	11.00	30.2	-170.0	LSR-V	1	7301	20:58
08.08	7.00	28.8	45.9	CMB-H	1	7769	14:17
08.67	45.75	29.8	18.4	CMB-H	1	7159+	06:57
08.95	-15.75	75.4	85.0	GBC-V	1	7452+	11:59
10.43	-21.25	29.0	154.0	LSR-H	1	7481+	11:34
11.23	58.00	28.4	-34.4	GBC-V	1	7230	04:52
14.30	57.50	31.8	-134.6	CMB-H	1	7228	08:04
14.65	46.50	31.8	25.1	GBC-H	1	7164	12:36
15.47	-18.00	28.2	185.8	LSR-H	1	7599+	08:51
17.10	2.00	29.2	83.8	GBC-V	1	7351	02:47
18.05	23.50	28.0	99.8	GBC-V	1	7061	22:45
18.37	-19.50	52.8	-169.2	GBC-H	1	7467	20:24
18.45	38.50	28.2	0.4	LSR-H	1	7127	18:49
18.67	-23.25	44.4	9.6	CMB-H	1	7493+	18:59
18.68	-22.25	28.8	-1.0	LSR-H	1	7565+	14:17
19.18	-0.50	28.0	-73.7	GBC-H	1	7699	06:00
19.67	-23.00	29.0	66.4	CMB-H	1	7560	15:36
20.03	30.75	33.2	-31.0	GBC-H	1	7092	22:41
RUN C: 1420 MHz							
01.70	33.5	28.8	-15.9	LSR-H	3	8014+	15:47
02.90	32.0	30.2	197.1	LSR-V	1	8022+	16:28
03.10	58.0	224.0	-169.6	LSR-H	1	7847+	04:12
12.32	16.0	29.0	-115.0	CMB-H	1	8160+	16:49
12.73	-12.5	30.6	152.3	CMB-H	1	8364+	03:51
15.55	17.0	28.6	-50.1	GBC-V	1	8154+	20:26
19.57	47.5	35.6	-164.6	LSR-H	1	7916	16:06
23.72	8.5	33.0	-28.5	LSR-V	2	8216+	00:35

^a At epoch of observation.

^b In units of average power per channel; assuming noise statistics, the strongest expected signal is 31.7 in these units.

^c kHz offset from nominal observing frequency.

^d CMB = cosmic microwave background rest frame; GBC = Galactic barycenter; LSR = local standard of rest; H = horizontal (EW); V = vertical (NS).

^e 1 = single channel peak; 2 = <10 channel peak; 3 = ~ 20 channel peak; 4 = wide peak.

^f Calendar days since JD 2,440,000 (1968 May 23); a "+" symbol signifies that the same declination was observed on 2 consecutive days.

southern horizon rendered such data worthless, and simply shut the system down when the antenna was parked. The cluster of points at high declination at the end of run A was an attempt to follow up some interesting events, which in retrospect were probably interference that was insufficiently rejected by the Doppler chirp, which is ineffective at high declination. In subsequent runs we therefore limited the declination coverage to $-30^\circ < \delta < +60^\circ$.

As remarked above, we have found 37 narrow and strong spectral features during our 5 years of observations; none of these events was detected in adjacent integrations (i.e., within ~ 3 minutes), and none was detected again at the same sky coordinate in either the next day's (transit) reobservation, or during subsequent sidereal tracking (manual) reobservation. Thus we were unable to obtain convincing evidence of these

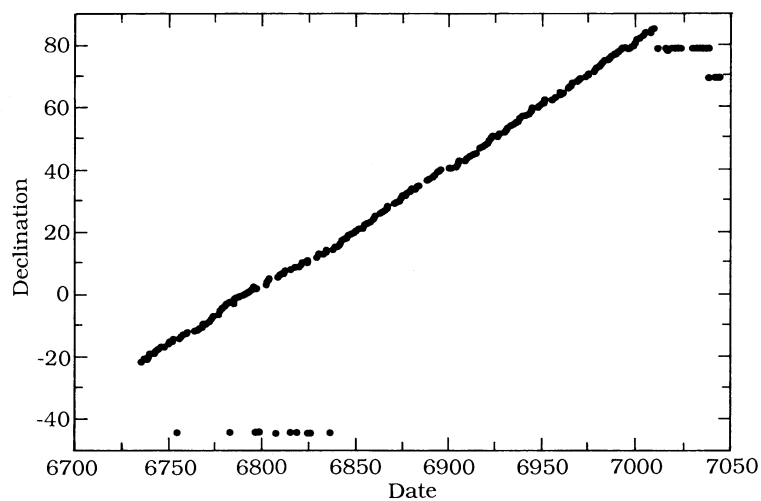


FIG. 3a

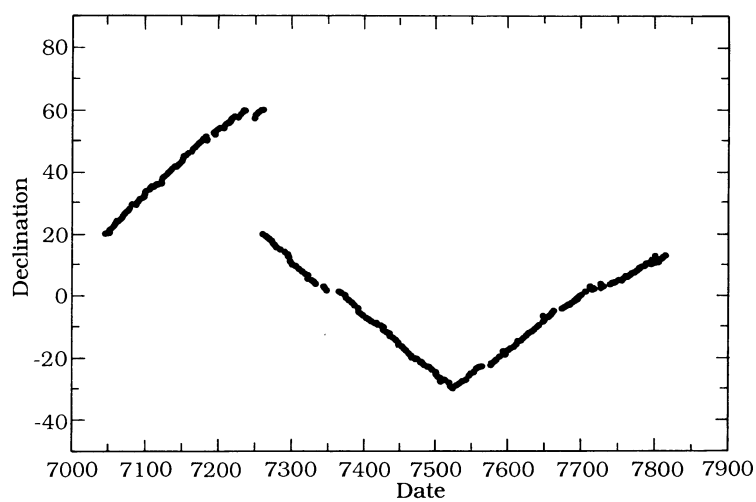


FIG. 3b

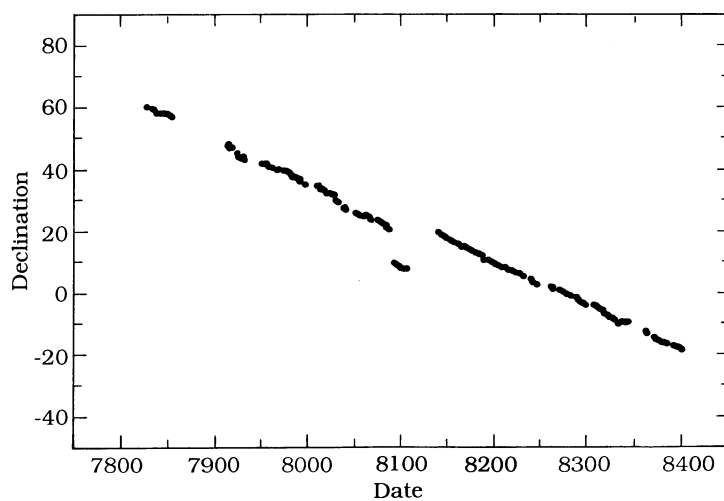


FIG. 3c

FIG. 3.—Declination coverage of META vs. Julian date (2,440,000 subtracted). The durations are 308 days, 783 days, and 572 days, respectively. Runs A and C are at 1420 MHz, run B at 2840 MHz.

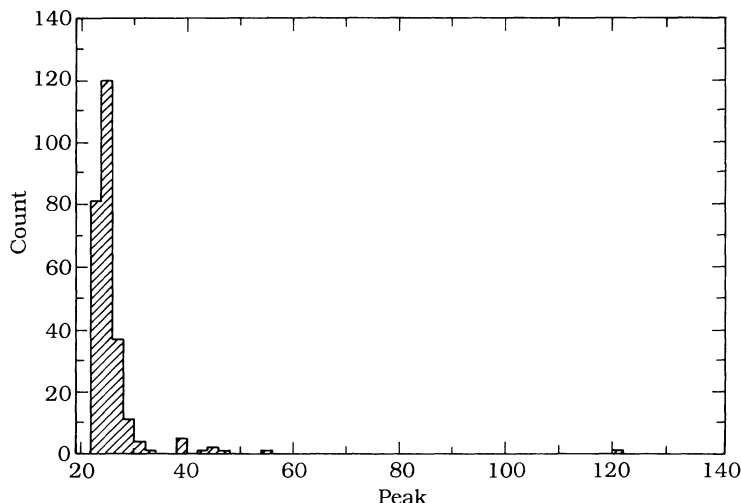


FIG. 4.—Histogram of isolated narrow peaks for run A, beginning at edge of “noise tail,” in units of average power per bin, P_0

signals as distant sources. Figure 4 is an intensity histogram of such events for run A, while Figures 5a–5b plot the celestial coordinates of narrow spectral events, again from run A, with two signal strength thresholds. The lower threshold (Fig. 5a: $22P_0$) is at the fringe of the noise tail, and presumably is dominated by statistical fluctuations. In Figure 5 we have used open symbols to indicate “resolved” spectral features, i.e., those that are broader than 0.05 Hz. The dashed line is the Galactic plane. Figures 6a–6c and 7a–7c are corresponding plots (at three successively higher thresholds) for runs B and C. Table 2 lists coordinates and characteristics of the events plotted in Figures 5b, 6b, and 7b. The strongest signal expected in $N = 6 \times 10^{13}$ samples (the full 5 year data set) on the basis of noise statistics alone is $P = P_0 \ln N = 31.7P_0$. Of the 37 entries in Table 2, 11 exceed this threshold, five by a significant amount and three by more than a factor of 2.

When preparing the plots of these latter events of higher signal strength, we looked closely for evidence of interference by terrestrial signals. After all, these 37 events represent the minuscule residue remaining after 6×10^{13} spectral channels have been subjected to the strict requirements of the detection algorithms (a narrow-band carrier, displaying expected Doppler chirp and sidereal drift, etc.); they amount to less than one part in 10^{12} of the data. At this level it should not be surprising, therefore, if there are subtle regularities, or other systematic pathologies. In fact, a careful look at the 74 candidate events initially remaining showed clear evidence of terrestrial interference in 37 cases, which we therefore omitted from Table 2 (and the corresponding plots in Figures 5b, 6b–6c, and 7b–7c). The clearest symptoms (often present in combination) were (1) the presence of a signal for a time duration much longer than the sidereal drift time through the beam diameter, and (2) a characteristic “marching peak” frequency progression through successive runs, corresponding precisely to the reception, by our agile receiver, of a signal of fixed *terrestrial* frequency (Fig. 8). Of the 37 events that we eliminated, 31 displayed one of these symptoms (and 16 displayed both); for every event displaying “marching peaks” we verified, by actual reenactment, that the observed frequency step size agreed in sign and magnitude with the deliberate receiver frequency programming, as illustrated in Figure 8. In a smaller number of cases we observed (3) the presence of approximately equal

signal power at equal positive and negative frequencies (signal leakage at baseband, after quadrature mixing), (4) signals with identical baseband frequencies during consecutive observations in different reference frames (signal leakage at baseband, again), (5) spurious detection during the initial 2 minutes of operation (during which the signal pipeline must be flushed), or (6) an error, found by the system’s array of redundant processors, in the processor board reporting the detection. This last category—processor error—accounted for four of the 37 events finally eliminated, which included some with the largest peak power ($38P_0$, $120P_0$, and two peaks larger than $1000P_0$). We note that the redundant checking scheme samples only $\frac{1}{8}$ of the operating processors at any time, and thus intermittent processor errors, not detected by the system, could be responsible for many of the events remaining in Table 2. Of the four known processor errors, two were detected while reporting their large spectral peaks, and two were detected during subsequent confirming spectra (within 2 minutes).

The events remaining in Table 2 (and plotted in Figs. 5b, 6b, and 7b) are those one in 10^{12} spectral channels that survived this inspection. Every event is isolated: all instances of “immediate” redetection, i.e., all signals that were initially seen to recur within the time interval during which a celestial source remains within the antenna beam, were found to exhibit fixed terrestrial or baseband frequency, and were therefore ascribed to terrestrial interference. Although it is not surprising to find a residue of nonreproducible events that defy explanation, we are puzzled by the fact that—if they are due to terrestrial interference—they (along with most of the 37 events we eliminated) do not display the characteristic frequency chirp that a terrestrial carrier must have. Within this group, events exhibiting horizontal polarization are more prevalent than those with vertical polarization (24 to 13), but the results are probably not statistically significant, given that no special effort was made to match the performance of the amplifiers and feeds for the two polarizations. The incidence of events observed in the respective inertial frames are uniform, with events observed in the LSR, GBC, and CMB inertial frames totaling 12, 14, and 11, respectively. As might be expected, events are rarer in the protected (21 cm) band of runs A and C (0.019 and 0.014 per day, respectively) than in the unprotected band of run B (0.028 per day).

The meaning of “extrastatistical” deserves some explanation, in the context of Table 2. In addition to requiring a narrow spectral feature, we somewhat arbitrarily set the received power threshold for inclusion in the table at $28P_0$, a value that should be exceeded ~ 8 times per year if the distribution of spectral power follows the exact exponential law discussed in § 3. Thus, at least some of the events listed in Table 2 are to be expected statistically, as the tail of the distribution. In this sense, the events with $28P_0 \leq P \leq 33P_0$ follow rather closely the expected distribution, and only events with $P > 33P_0$ are truly “extrastatistical,” meaning not plausibly assignable to a statistical fluctuation. This subset contains

eight events (22% of the 37 events included in Table 2), the strongest at $224P_0$ and $747P_0$. We chose the lower threshold in order not to exclude from the table possible signals that lie close to the statistical cutoff.

In examining these plots, we see no obvious correlation from run to run. Those events exceeding a threshold of $34P_0$ (the four points in Figure 6c and the two points in Figure 7c) tend to lie in or near the Galactic plane. In addition, four of the six strongest signals in run A (Fig. 5b: threshold of $28P_0$) are correlated with the Galactic plane. While this may be due to the statistics of small numbers, it is just what would be expected for transmissions from civilizations within the Milky

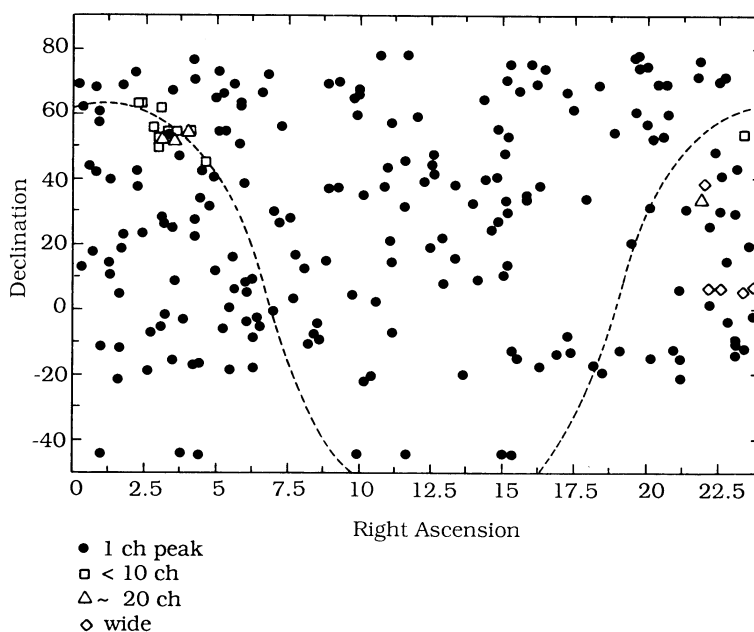


FIG. 5a

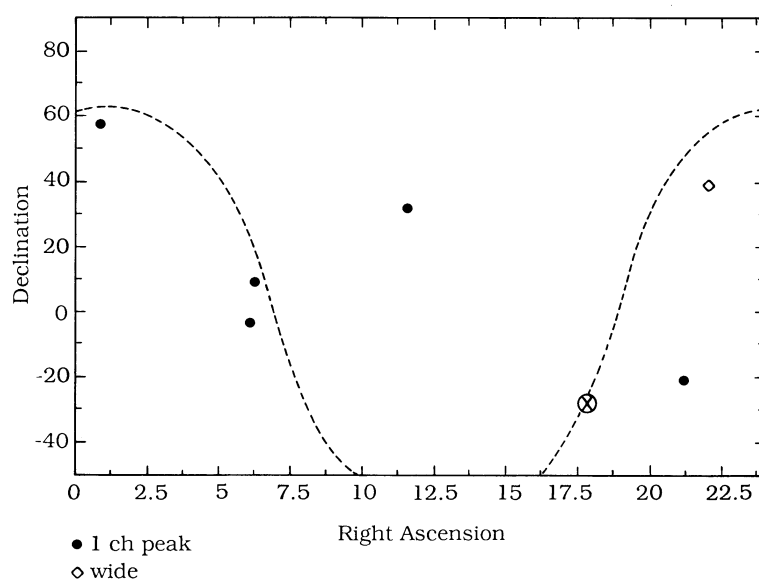


FIG. 5b

FIG. 5.—Coordinates of strong spectral features for run A (1420 MHz). Thresholds are (a) $22P_0$ and (b) $28P_0$. The dashed line is the Galactic plane; \otimes is the Galactic center.

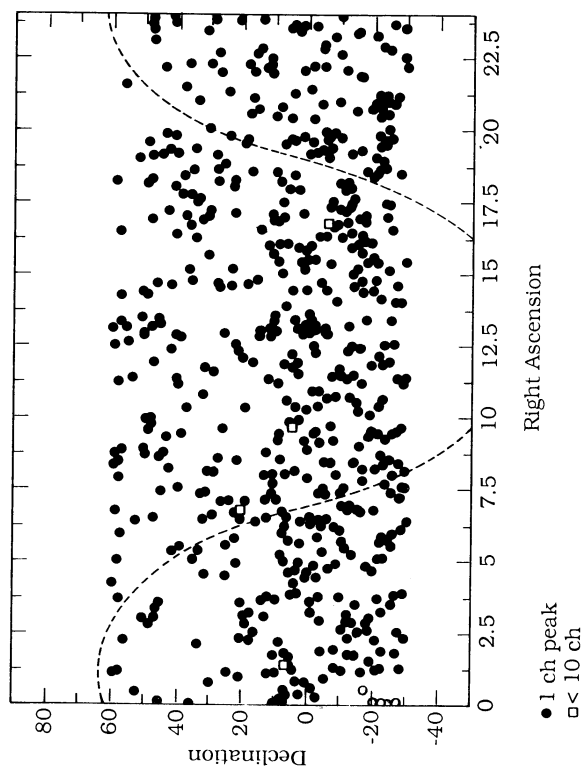


FIG. 6a

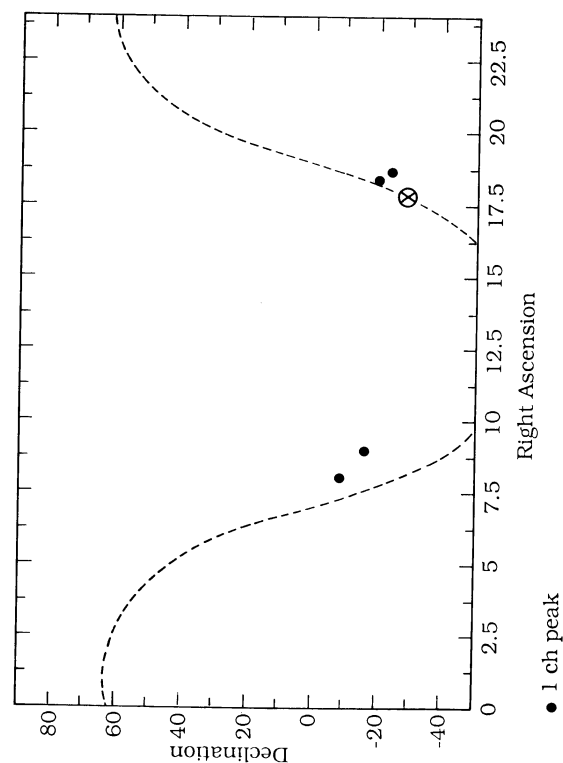


FIG. 6c

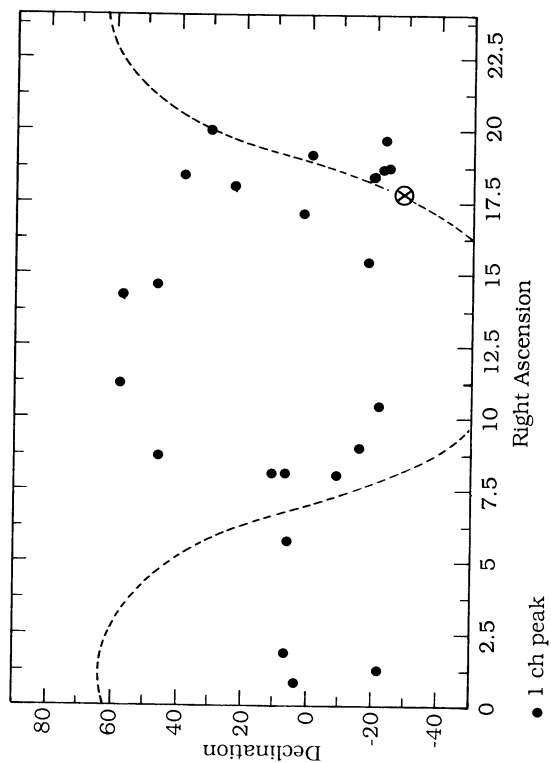


FIG. 6b

FIG. 6.—Coordinates of strong spectral features for run B (2840 MHz). Thresholds are (a) $22P_0$; (b) $28P_0$; (c) $34P_0$. The dashed line is the Galactic plane; \otimes is the Galactic center.

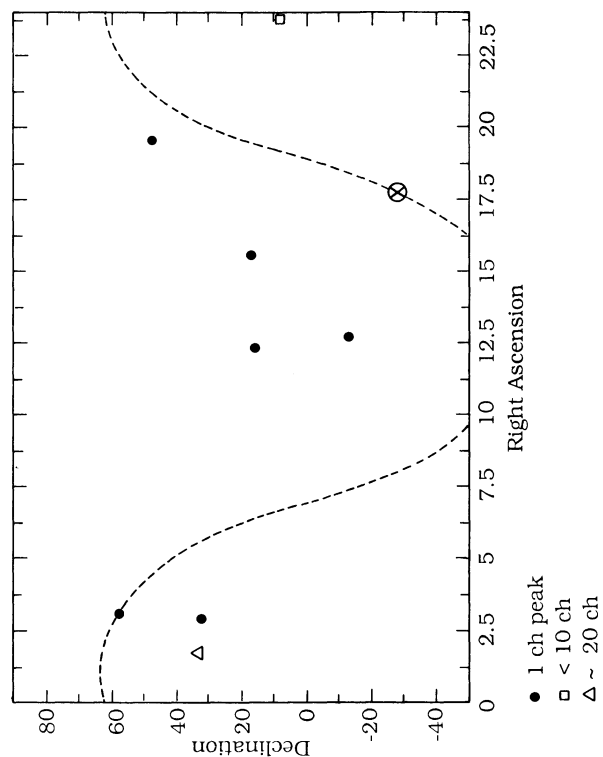


FIG. 7b

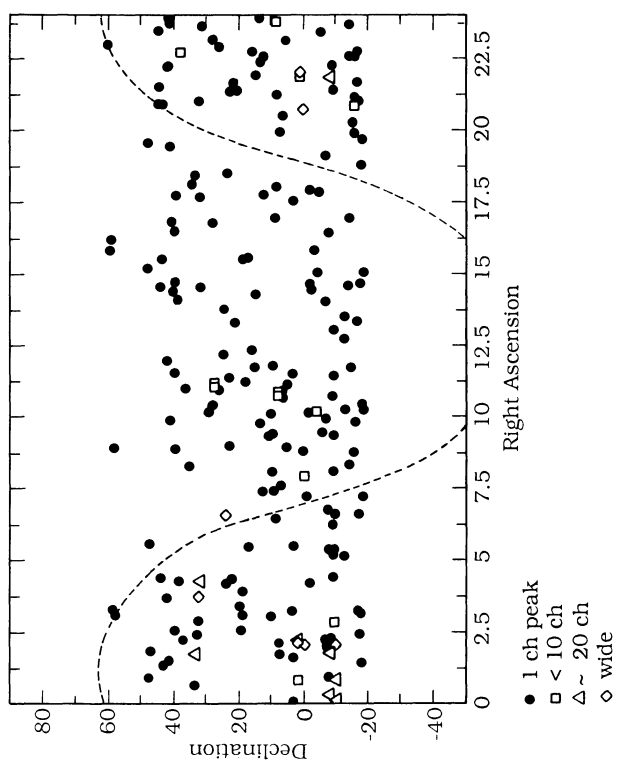


FIG. 7a

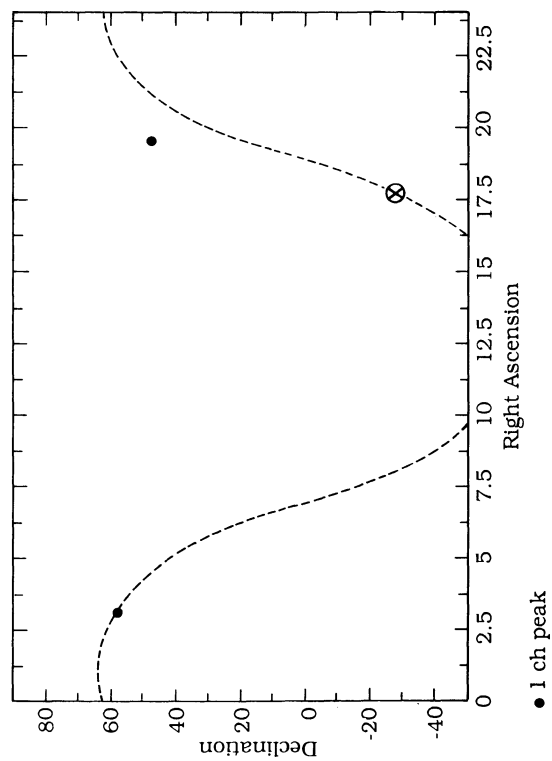


FIG. 7c

FIG. 7.—Coordinates of strong spectral features for run C (1420 MHz). Thresholds are (a) $22P_0$; (b) $28P_0$; (c) $34P_0$. The dashed line is the Galactic plane; \otimes is the Galactic center.

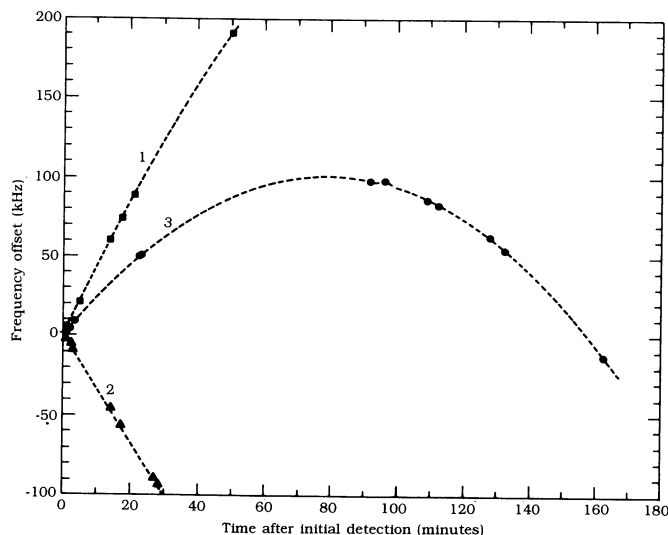


FIG. 8.—Examples of signals whose observed frequency progression with time corresponds to that of the META receiver, thus establishing the source as a fixed terrestrial frequency. The points plot persistent observed signals with peak spectral feature $>22P_0$, graphed relative to time and frequency of first detection. The dashed lines are META's programmed frequency, as calculated at the epoch of observation, relative to the time of first detection. The particular observations (all in the CMB frame) are (1) 1991 March 13, $\delta = -8^\circ$; (2) 1987 January 14, $\delta = 6^\circ$; (3) 1987 May 14, $\delta = 52^\circ$. The programmed steps in received frequency arise primarily from the diurnal rotation of the antenna's beam direction, whose changed dot product with Earth's velocity vector (with respect to the selected inertial frame) necessitates a step in receiver frequency of as much as 2 kHz (at 1.4 GHz), from one 20 s integration to the next; note that this stepwise jump is nearly three orders of magnitude larger than the continuous "Doppler chirp" described earlier, because Earth's velocity with respect to both the GBC and CMB frames is about three orders of magnitude greater than Earth's surface velocity of rotation. Note that the dotted curves do not represent a fit to the data, but rather an independently derived function with one adjustable parameter (vertical offset); for data set No. 3, however, the time axis was offset by 25 s, a minor adjustment consistent with the accuracy of the computer's real-time clock (± 1 minute).

Way, or from a previously unknown astrophysical source of narrow-band radio emission distributed with Galactic stars, gas, and dust. Note that the declination coverage is not completely uniform (see Fig. 3), which is reflected in the density of points in the scatter plots of Figures 5–7.

The observing program of run C differed from that of run A in only two ways: first, the dwell time per declination was increased to 2 days (and sometimes three), evident in the slopes in Figure 3. Second, the definition of the cosmic microwave background rest frame was refined, based on improved observational data. Specifically, the assumed velocity and direction of the heliocentric motion with respect to the microwave background frame was changed from a preliminary value of 342 km s^{-1} toward $\alpha = 11^{\text{h}}18^{\text{m}}$, $\delta = -5^\circ$ to the currently accepted value of 362 km s^{-1} toward $\alpha = 11^{\text{h}}12^{\text{m}}$, $\delta = -7^\circ$ on 1988 August 21 (JD 2,447,395), during run B. Note that this change corresponds to significantly less than META's instantaneous bandwidth, namely, a maximum offset of received frequency of 100 kHz (in a band of 400 kHz). (The values for the other two frames were unchanged: for the GBC we used $v = 210 \text{ km s}^{-1}$, $\alpha = 21^{\text{h}}32^{\text{m}}51^{\text{s}}$, $\delta = +48^\circ47'48''$; for the combined LSR/heliocenter we used $v = 10 \text{ km s}^{-1}$, $\alpha = 18^{\text{h}}$, $\delta = +30^\circ$.)

During September and October of 1991 we carried out extensive reobservations of a superset of the Galactic plane

events plotted in Figure 5b: each of 13 source positions was observed in tracking mode, covering the normal suite of reference frames and antenna polarizations, for an average uninterrupted duration of $4^{\text{h}}10^{\text{m}}$. There were no extrastatistical events (i.e., $P > P_0 \ln N$) during some 54 hours of such observations, which included every Galactic plane source position that had exhibited extrastatistical events during its ~ 2 minutes of original observation in run A. During 1993 February we reobserved (at H I only) the six strongest peaks in Table 2, with similar results.

In Figure 9 we have plotted peak intensity versus time of day (in UT), in order to display any diurnal regularity that might indicate a local source of interference. There is no obvious clustering, although one might argue that the events occur with somewhat greater likelihood during working hours (13:00–22:00 UT).

5. DISCUSSION

The foregoing results can be summarized, without judgment, as follows:

1. META's observation interval of each potential source is ~ 2 minutes yr^{-1} (duty cycle $= 4 \times 10^{-6}$), during which it would reliably ($30P_0$) detect a flux of $0.7\text{--}13 \times 10^{-23} \text{ W m}^{-2}$ (corresponding to an effective isotropic radiated power [EIRP] of $0.8\text{--}15 \times 10^{16} \text{ W}$ at a distance of 1000 light years), if transmitted at a fixed frequency within $\pm 200 \text{ kHz}$ of the selected frequency (either H I or 2 H I), as seen in one of three inertial frames (LSR/heliocenter, Galactic barycenter, cosmic microwave background). For comparison, the terrestrial transmitter of highest microwave brightness (Arecibo S-band planetary radar) has an EIRP of $7 \times 10^{12} \text{ W}$ (soon to become $2.4 \times 10^{13} \text{ W}$).

2. During 5 years of observations, there have been 37 spectral peaks that could be good candidates for an ETI signal of the above description (strong, narrow, inband); eight of these lie beyond the statistical noise tail. None has repeated during immediate reobservation (beginning at $t_0 + 40 \text{ s}$, and continuing for ≈ 3 minutes), during a subsequent daily reobservation in transit mode ($t_0 + 1$ day), in a later reobservation in tracking mode ($t_0 + 6$ months, ≥ 30 minutes duration), nor in a recent set of tracking reobservations of longer duration ($t_0 + 5$ years, $4^{\text{h}}10^{\text{m}}$ average duration per candidate). At the highest threshold of signal power there is a rough but suggestive correlation of candidate signals with the Galactic plane (see below).

We now consider two antithetical hypotheses, namely (1) that all of these extrastatistical events are signals of extraterrestrial origin, and (2) that none are.

5.1. If All 1420 MHz Events are ETI Signals

The hypothesis that these events represent a substantial number of extraterrestrial radio beacons of low duty cycle can be challenged by the following argument: The lack of any confirming observations ≈ 1 minute after the initial event means that the duration of the putative signals is at most 1.5 minutes; but a spectrally narrow detection (i.e., power confined to 1 or 2 spectral channels) requires that the signal be present during the entire 20 s integration time τ_i (otherwise one would observe a $\text{sinc}^2 f$ rectangular pulse broadening). Thus the hypothesis not only constrains the durations of transmitted signal τ_i (to $\tau_i = 20 \text{ s} < \tau_i < 100 \text{ s}$), but also predicts the *distribution* of observed carrier durations within the integration window, assuming random alignment of signal and integration

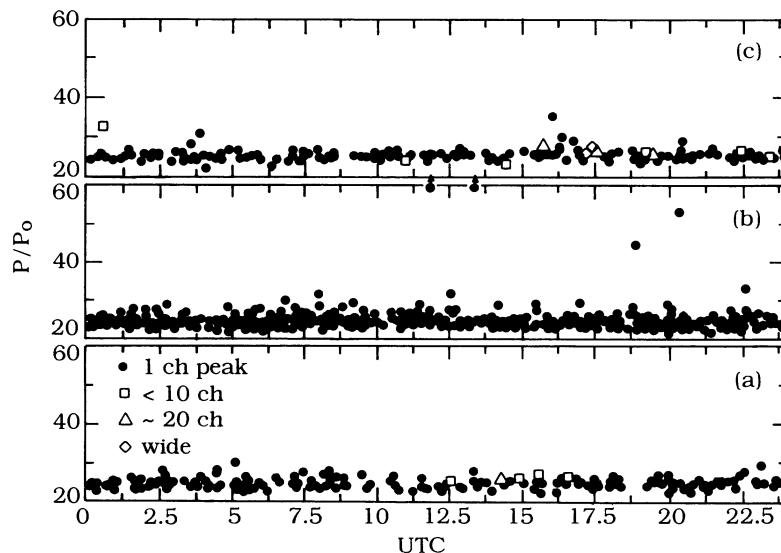


FIG. 9.—Strong spectral features vs. Universal Time. (a) Run A (1420 MHz); (b) run B (2840 MHz); (c) run C (1420 MHz)

intervals: $P(\tau, \tau + d\tau) = 1/\tau_i$ for $\tau < \tau_i$, otherwise $P(\tau_i) = 1 - \tau_i/\tau_i$, where the transmitted carrier duration τ_i is assumed constant. In other words, there is a uniform likelihood for all observed carrier durations up to the integration interval, with an excess likelihood of signals completely filling the integration window if the transmitted pulse duration is greater than the integration interval. Let us refer to this prediction of an extended distribution of observed spectral widths from intermittent carrier transmissions as “time-overlap broadening.”

This appears to be inconsistent with the detection events seen at 2 H I (Fig. 6), which are entirely of the 1- or 2 channel kind, and also with the H I events seen at higher thresholds and also surviving the interference criteria of § 4 (Figs. 5b and 7c), which also do not display time-overlap broadening. In fact, only the low-threshold events of run C (Fig. 7a) display a significant proportion of broadened events. In considering this argument, however, it is important to note that the *observed* distribution of signal durations (i.e., the distribution of those whose highest channel exceeds some threshold) will be skewed in favor of long-duration signals, because for signals with incomplete overlap τ_0 with the integration window the resulting magnitude of the peak spectral channel is reduced by the combined effects of (1) reduced total signal energy within the integration window, and (2) dilution of that total signal energy over a larger number ($\approx \tau_i/\tau_0$) of spectral channels. Thus a preponderance of spectrally unresolved events is not a priori inconsistent with time-overlap broadening, particularly if the strongest detected events do not greatly exceed the detection threshold.

The time-overlap broadening argument further depends crucially on the efficacy of reobservation. In particular, for any reasonable luminosity distribution a real (and continuously on) signal will tend to be first detected when the search system is close to maximum sensitivity (beam center, bin center), with the likelihood that follow-on observations will have to contend with reduced signal levels (as the source transits out of the beam, falls between frequency bins, etc.). These effects are not negligible: a signal first detected at $40P_0$ close to beam center and bin center will be 3 dB down at the time of first reobservation, due to beam transit, and quite possibly another 3 dB

down if the initial observation was close to the center of a frequency bin; thus it might escape confirmation at its reobservation level of $10P_0$. Thus a set of observations dominated by unresolved spectral peaks, the strongest of which exceed the detection threshold by only a modest factor, could be consistent with the detection of signals from a set of narrow-band radio beacons. We have not explored this scenario further; it may argue for future search strategies designed to achieve uniform sensitivity.

We note that the physics of propagation through the Galactic plasma of radio signals from narrow-band point-source emitters produces large amplitude variability (“scintillation”) of received signal strength. Cordes & Lazio (1992) have modeled the process, using data from pulsar scintillation, and find that scintillation works most often to make a marginal signal undetectable, and more rarely to make an otherwise submarginal signal detectable. For a planetary transverse relative velocity $\approx 10 \text{ km s}^{-1}$ and a dispersion measure typical of the Galactic plane beyond 80 pc, characteristic scintillation time scales are minutes to hours (the shorter time scales corresponding to sources in the Galactic plane at distances greater than a kiloparsec, and the longer time scales to closer sources). During a given scintillation event, the intensity remains roughly constant. Thus, if our Galactic plane events were due to submarginal Galactic transmitters a few kiloparsecs distant, we would expect them sometimes to be repeatable after 3 minutes, but rarely during short observations made days or years later.

The probability distribution function (Cordes & Lazio 1992) for scintillation amplification of received signal power by a factor g is just $\exp(-g)$. This means that $g = 10$ or 20 will occur occasionally, but $g \geq 100$ never. If one were to accept the META events as real sources, enhanced by scintillation, one might well ask why transmitters of (presumably) widely differing powers and distances across the Galaxy have their signal strengths tuned so as to be brought just up to current detectability on Earth. No Galactic conspiracy seems needed, however: no one has detected narrow-band extraterrestrial signals at fluxes $\geq 10^{-23} \text{ W m}^{-2}$ (of the searches tabulated [Tarter 1993], only Serendip II, Sentinel, and META I and II

have the combination of sky coverage and sensitivity required). Thus if a significant number of our events are ETI signals, they would most likely be the strongest and/or nearest of a wide range of distant transmitters. Note that if intermittency is in fact due to scintillation, it is strong evidence that the transmitters lie well beyond the solar system.

For the above reasons we believe that the initial hypothesis of this section—that the events we have seen arise from a large number of extraterrestrial beacons of low duty cycle—however improbable, cannot be conclusively ruled out. What could we deduce if we were willing to take the view (admittedly implausible) that *all* of the events seen by META that were not eliminated by the criteria of § 4 (i.e., those listed in Table 2), are due to extraterrestrial transmitters? Given that META's duty cycle is 4×10^{-6} , and given the above argument that the signal duration is at least as long as the integration interval but rarely exceeds the time for a point in the sky to drift through the antenna beam, it follows that there are of order 2×10^6 transmitting sites detectable by META in the portion of the sky it has surveyed (i.e., merely the ratio of the number of events per sky survey divided by META's duty cycle). This is of the same order as some estimates (e.g., Shklovskii & Sagan 1966) of the number of advanced civilizations; such estimates are of course highly speculative, and we mention them here only to suggest that a large number of transmitting sites are not to be rejected a priori. Note additionally that if just *one* of the events seen by META is due to an extraterrestrial transmitter, then the corresponding figure becomes 5×10^4 detectable transmitters.

We know of no astrophysical process that could account for the narrow-band candidate signals META has recorded, and we have been unable to find any correlation of source positions with unusual astrophysical objects.

5.2. If No 1420 MHz Events are ETI Signals

Extraordinary claims require extraordinary evidence. Given the nature of the occasional strong spectral features, we have no choice but to continue to insist that only a signal that is found to repeat, and that displays constant sidereal coordinates, can be considered a viable candidate. Thus—no matter how provocative the signal characteristics or their correlation with the Galactic plane—we have not found convincing evidence of radio signals of intelligent extraterrestrial origin.

If, then, the result of 5 years of continuous observation is a complete absence of narrow-band signals, what can be concluded from this null result? As we shall see, it may put the notion of communicating “supercivilizations” in some jeopardy. Let us adopt Kardashev-like definitions (Kardashev 1964) of energetically extravagant civilizations: A “Type I” civilization has available power equal to solar insolation on Earth, in round numbers 10^{17} W (for which Bania has coined the acronym “twit”: total watts incident, terrestrial), and a “Type II” civilization has harnessed a solar luminosity, 10^{26} W. To these let us add ourselves, a modest civilization of “Type 0,” with total power resources of a mere 10^{13} W (only 1 part in 10^8 of which is devoted to interstellar communication). Note that Kardashev's Type I is our Type 0—he gave no standing to civilizations that exploit their full planetary insolation, which we call Type I.

If we now confine our attention to supercivilizations that engage in transmissions of radio-frequency carriers that fall within META's bandpass (i.e., Doppler-precompensated beacons at H I or its second harmonic), and furthermore assume that they extravagantly devote a major fraction of their

available power to the task of interstellar communication, our negative result allows us to set the following limits on the number N of such civilizations in our galaxy (where ϵ is the Earth-incident duty-cycle of transmission, i.e., the fraction of time spent transmitting in our direction):

For Type 0: $N\epsilon < 1$ out to 7 pc (≈ 15 Sun-like stars) for an isotropic beacon. $N\epsilon < 1$ for the entire Galaxy ($\approx 10^{11}$ Sun-like stars) for directed beacon transmissions, with transmitting antenna gain $G_t \approx 70$ dB.

For Type I: $N\epsilon < 1$ out to 700 pc ($\approx 10^7$ Sun-like stars) for an isotropic beacon. $N\epsilon < 1$ for the entire Galaxy ($\approx 10^{11}$ Sun-like stars) for directed beacon transmissions, $G_t \approx 30$ dB.

For Type II: $N\epsilon < 1$ out to 22 Mpc ($\approx 10^{11}$ Sun-like stars in the Galaxy, plus $\approx 10^{14}$ in neighboring galaxies) for an isotropic beacon. (Type II civilizations do not need directional antennas!)

We have used a value of 10^{-2} pc $^{-3}$ for the density of nearby Sun-like stars. Only when $\epsilon > 10^{-6}$ do these directed transmission limits on N fall below possibly optimistic estimates (Shklovskii & Sagan 1966; Sagan 1973) of N for Types 0 and I civilizations. When considering *directed* beacons, two scenarios suggest themselves, namely (1) the transmitting civilization irradiates those target stars that it deems most likely to harbor intelligent life, based upon astronomical observations, or (2) the transmitting civilization transmits only toward stars from which it has already received radio signals; we might call these strategies *preemptive* and *responsive*, respectively. Given Earth's short history of radio transmissions (whose expanding spherical wavefront has reached only ≈ 15 pc), META has set no important limits on the abundance of Types 0 or I civilizations that adhere to a responsive beacon strategy; however, the constraints on such civilizations with preemptive strategies are stringent.

We can set corresponding limits on *distant* (extragalactic) powerful beacons (necessarily preemptive), again assuming that the signal as received on Earth would fall within META's bandpass (see below for further discussion on META's source volume). If we take the number density of potential civilizations to be comparable to the number density of stars, say $n = 3 \times 10^{-58}$ m $^{-3}$ (or 10^{10} Mpc $^{-3}$), then the fraction of sites transmitting, multiplied by their duty cycle, lies below the line plotted in Figure 10. If powerful transmissions at H I-related frequencies constitute one of the activities of Type II civilizations, then such civilizations seem to be very rare.

5.3. META's Source Volume

Serious consideration of supercivilizations takes us out to cosmological distances, with correspondingly large redshifts. This puts an interesting limit on META's source volume, because a beacon signal that is transmitted at a preferred frequency as seen in the local inertial frame in which the microwave background radiation is isotropic will not be seen at the same frequency when it arrives at a distant receiver, relative to *its* microwave background rest frame, but rather will partake of the general cosmological redshift. Of course, the transmitting civilization could precompensate the frequency of a directed beacon to allow for the cosmological expansion, given knowledge of the receiver's distance; but let us imagine that no such compensation is made—perhaps because transmission is intended for a very large number of potential receivers at varied distances—and ask how META's finite bandwidth limits the potential source volume.

As an upper bound, we note that a Type II civilization radiating its 10^{26} W as an isotropic beacon at a preferred frequency

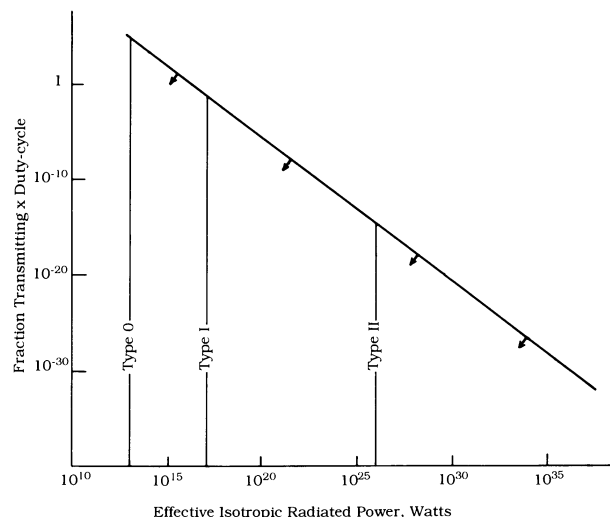


FIG. 10.—Constraint on distant powerful transmitting civilizations if no H I events are ETI signals, neglecting cosmological redshifts.

(an activity that gives new meaning to the term extravagance) would be detectable out to 36 Mpc, within which there are something like 10^{14} stars. However, distant sources are cosmologically redshifted, to first order given by $\Delta f = f_0(v/c) = f_0(H_0 R/c)$, leading to a bandwidth-limited range $R = (\Delta f/f_0)c/H_0$, where H_0 is the Hubble constant, which we take to be $50 \text{ km s}^{-1} \text{ Mpc}^{-1}$. META's bandwidth ($\Delta f = \pm 200 \text{ kHz}$) thus corresponds to $R = 0.8 \text{ Mpc}$, meaning that only Galactic sources are in-band ($\approx 10^{11}$ stars). Thus we must qualify our previous conclusions about the nonprevalence of distant supercivilizations (e.g., Fig. 10) with the observation that we have assumed that they have adjusted their transmission frequency such that their signal arrives in our Galaxy at the preferred frequency. This they could do by observing our Galactic spectral lines and applying the inverse correction (thus ensuring that the signal arrives correctly shifted in the Galactic barycentric frame), or by applying an offset designed to cancel the cosmological shift (thus ensuring that the signal arrives correctly shifted in our microwave background frame). The limits in Figure 10 apply only to supercivilizations with such transmitting strategies. But if there were a large number of supercivilizations, it seems surprising that none of them would adopt such a strategy. We argue that the limits set by META on supercivilizations transmitting preemptively at H I are stringent also.

5.4. Probable Origin of Extrastatistical Events

If we assume that none of the events in Table 2 represent narrow-band sources of extraterrestrial origin, we are still faced with the problem of their origin. As we remarked in § 4, the events with signal power less than $33P_0$ obey the expected exponential statistics of random signals, leaving just eight “extrastatistical” events. Of these, three have signal power close to the noise tail (between $33P_0$ and $36P_0$), leaving five events—an average of one per year—that are clearly separated (they have 44, 53, 75, 224, and 747 times the mean channel power P_0). The absence of “chirp broadening” in these events seems to rule out their explanation as fixed terrestrial carriers, but still allows several mundane possibilities: (1) If terrestrial microwave carriers display an ensemble of drift rates at the level of parts in 10^9 per second, these events could represent the enhanced response of the chirp spectrometer to that subset of

the in-band ensemble with approximately the correct drift rate. (2) The acceleration of a satellite in solar orbit at greater than 3.5 AU broadens a transmitted carrier by less than META's resolution bandwidth; thus such a spacecraft with a stable carrier or spur in META's bandpass, positioned in the general direction of the telescope beam, could, in principle, generate a candidate event. (3) As explained in § 4, the fact that known processor errors contributed four candidates of the additional 37 now eliminated from Table 2 suggests that intermittent and undetected processor error could be responsible for some of the remaining events. One plausible mechanism is occasional “soft” errors in dynamic RAM memory (which comprise 6912 of META's 20,000 integrated circuits) caused by α particles. These occur (Hester 1992; Yerazunis 1992) in the kind of memory chips used in META (64 K DRAM) at a rate of ~ 500 FITs (“failure in time,” defined as 1 error per 10^9 chip hours). Using this rate, one can estimate that there ought to be ~ 125 soft errors during the 4×10^4 operating hours of META. To this count we apply factors of $\frac{1}{2}$, $\frac{1}{2}$, and $\frac{1}{8}$, respectively, to account for the fact that only half act in a direction to *increase* the size of a signal, that the error must be in the upper half of the integer to create a large enough error amplitude, and that, in order to create an isolated spectral feature, the error must occur approximately during the last two of the 16 “butterflies” that comprise the Fourier transform. Thus we estimate that soft memory errors might account for ≈ 4 false peaks during the 5 years of observations reported here. Given that our estimate is unlikely to be accurate to better than a factor of 2, this error source could account for some of the events remaining in Table 2, in addition to the four earlier candidate events that were removed from the table because of known processor errors that were detected by the redundant processor array. (4) A more mundane source of processor error is socket and connector contact degradation, which we have observed on some occasions as a source of processor unreliability. This is not surprising, given the fact that there are $\sim 2 \times 10^5$ socket pins and 2×10^4 backplane pins in the META system. It is difficult to quantify this error source, but from our experience we estimate that it might plausibly be responsible for a handful of the events in Table 2.

Of these alternatives, (1) and (2) seem rather unlikely as the source of more than an occasional entry in Table 2. On the other hand, (3) and (4)—processor errors—are known to have occurred, and plausible estimates include the possibility that all five events of substantial signal strength ($P > 36P_0$) are due to this cause. Furthermore, the explanation of the remaining (weaker) events in the table as expected statistical fluctuations seems altogether reasonable. Such an explanation is consistent with the premise of § 5.2, and with our claim that the result of this 5 year search is no compelling evidence of narrow-band signals of extraterrestrial origin.

Although the foregoing explanations of signal origins are consistent with the narrow and isolated nature of the spectral peaks, they do not explain the apparent correlation of strong signals with the Galactic plane which can be seen clearly in Figure 11, where we have plotted all 37 candidate events along with the visible Milky Way, the Galactic plane, and the Galactic Center. The large circles are the five strongest events ($P \geq 44P_0$).

6. RECOMMENDATIONS FOR FUTURE SEARCHES

The META project has demonstrated that megachannel SETI can be operated at a remote site, at low cost, and—if the frequency and spectral character of potential signals are severely

constrained—with excellent resistance to terrestrial interference. However, it has found a handful of narrow-band events that are puzzling—these strong base-band signals correctly mimic the Doppler chirp signature expected of a genuine extraterrestrial carrier as seen in Earth's rotating frame. Moreover, after terrestrial interference is winnowed out, the strongest spectrally unresolved sources are clustered near the plane of the Milky Way. It is a weakness of the META system that it is unable to track the source position of such a signal immediately, a weakness it shares with other carrier-seeking SETIs (a few of which, incidentally, have found similar unresolved and unexplained signals [Dixon & Tarter 1991]). *It is most important that future SETI systems are able to follow up candidate signal detections immediately, in order to resolve this kind of ambiguity.* An attractive alternative would consist of a pair of dedicated and widely separated observatories simultaneously observing the identical celestial coordinates (a mode we are trying, in cooperation with the recently installed "META II" receiver at the Argentine Institute for Radioastronomy near Buenos Aires).³

The need for rapid reobservation in SETI is, of course, a consequence of radio interference and other electronic transients. We note with concern the proliferation of communication systems in the important microwave region of the spectrum. Although some mitigation efforts can be successfully applied to terrestrial sources (reduced sidelobe feeds, shielding screens), interference from satellites is far more troublesome, owing to continually changing line-of-sight geometries, and the use of modulation schemes such as direct-sequence spread spectrum that can blanket many megahertz with spectral features. Satellite (and airborne) signals have haunted SETI efforts for 30 years; a recent set of observations was seriously jammed by the *Glonass* navigational satellite system (Heidmann, Biraud, & Tarter 1989). The future evolution of SETI, involving greater bandwidth and sensitivity, will have to contend with pervasive interference in unprotected bands. It is probably no exaggeration to say that radio frequency interference may be the greatest impediment to the eventual detection of extraterrestrial intelligence.

7. FOLLOW-ON SEARCHES

We have now devoted more than five years to continuous high-resolution SETI observations in the neighborhood of two preferred frequencies, including multiple observations at H 1. The search methodology, with its insistence on fixed narrow-band carriers in a guessable inertial frame, has discriminated well against terrestrial interference, in almost all instances rendering it both attenuated and recognizable. However, the search has failed in the most important way: despite some puzzling and provocative results, it has made no unambiguous detections of extraterrestrial radio transmitters.

It is clear that our searches are far from ideal, given their small total bandwidths (400 kHz), only moderate sensitivity (due to modest apertures and receiver noise temperature), low duty cycle, and insensitivity to signals other than carriers (e.g., pulses or chirps). Future searches, less narrowly constrained

and of higher sensitivity, are of great interest. In particular, the elegant parasitic Serendip III system now operating at Arecibo (Bowyer et al. 1992) explores a new frequency regime at very high sensitivity. And most importantly, the twin NASA strategies (Sky Survey and Targeted Search), which commenced observations 1992 October 12, with their combination of sensitivity, wide frequency coverage, and ability to detect carriers, pulses, chirps, and their combinations (Tarter 1991), clearly represent an enormous stride in comprehensive SETI; we hope they will shed light on the class of enigmatic signals reported here.

7.1. Waterhole Millihertz SETI

The benefits of high-resolution ($B \ll 1$ Hz) SETI (not implemented in the NASA program), especially in terms of rejection of interference, make it worthwhile to ask how such a strategy could be extended.

The obvious way to increase total bandwidth while maintaining high resolution is simply to increase the channel count. A *gigachannel* spectrum analyzer, for example, would cover 50 MHz of instantaneous bandwidth while retaining META's 0.05 Hz resolution. While such an analyzer would have been unrealizable a decade ago (it would have required 750,000 of the 64 K bit memory chips just then available), it is now possible. If we extrapolate current trends in memory density and price only modestly, we conclude that a gigachannel analyzer will require less than \$250 K in parts within 5 years, and that even a 6×10^9 channel high-resolution analyzer could be constructed with university labor and budgets within the decade. Such a spectrometer would cover 300 MHz instantaneous bandwidth (for example, the entire "waterhole" of 1.4–1.7 GHz, a favorable band for SETI that is bounded by the microwave emission lines of the dissociation products of water [Oliver & Billingham 1972; Morrison, Billingham, & Wolfe 1977]), at a resolution binwidth roughly matched to the properties of the Galaxy (Cordes & Lazio 1991). It is our intention to design and build such a spectrometer sometime during the 1990s.

7.2. 240 Megachannel Three-Beam SETI

Another approach to advanced high-resolution SETI is to gain total bandwidth by a more modest increase in channel count, combined with wider individual channels. We are currently constructing a search system to achieve 120 MHz of instantaneous bandwidth, in the form of 240 million channels of 0.5 Hz resolution. Interference rejection must now be achieved by some other route, since the chirp scheme used in META is no longer effective (with 0.5 Hz bins the chirp at H 1 during the 2 s integration is about $\frac{2}{3}$ of a bin). Davis (1990) has suggested the use of dual feed horns with a 2-channel receiver, in a meridian transit search (Fig. 12), to which we are adding a terrestrial nondirectional channel. A true celestial source will have a unique signature of "preceding/following"; ideally, each lobe would show a beam profile characteristic of the antenna's gain pattern, distorted perhaps by the effects of interstellar scintillation. (Even with distortion, however, the characteristic lobe alternation should be unmistakable; local interference simply does not move from one beam's sidelobes to the other's at sidereal rate, and in precisely such manner as to enter and then disappear from *all* sidelobes with the correct timing). Any signals that *do* satisfy the criteria of proper beam alternation, timing, and absence from the terrestrial antenna must, of course, ultimately satisfy the more stringent criteria of

³ For example, if we set a threshold of $P = 16P_0$, which generates approximately one event per 8.4 million-channel spectrum, and define a "coincidence" as a pair of events at the two observatories that lie within ± 10 frequency bins in the same 20 s observation, then noise statistics alone would generate ~ 4 coincidences per year. To achieve this same false-alarm rate at a single observing site requires a threshold of $28.8P_0$, or roughly half the sensitivity of coincident observations.

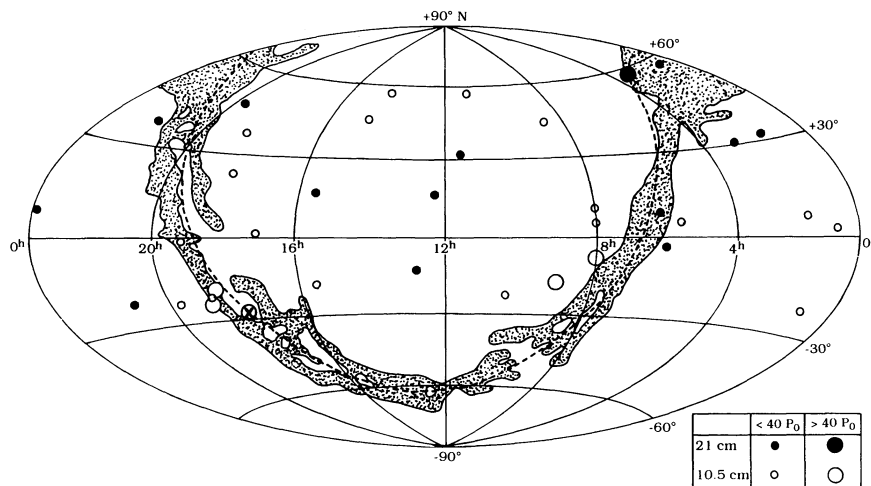


FIG. 11.—Events of Table 2, plotted on an equal-area projection of the sky. Filled circles are from runs A and C (1420 MHz), open circles from run B (2840 MHz). The five strongest events ($P \geq 44P_0$) are shown as larger circles. The stripping represents the visible Milky Way, and \otimes the Galactic center.

repeatability, sidereal drift, and observability by another observatory site.

Our design organizes the analyzer as a set of three simultaneous 80 megachannel analyzers (each of 40 MHz instantaneous bandwidth), two driven by focal-plane feedhorns, and one driven by a nondirectional terrestrial comparison antenna. By stepping the center frequency between each integration we cover the entire waterhole every 16 s. In the ≈ 2 minute interval for a potential source to drift through each stationary 0.5° antenna beam we would thus make eight simultaneous observations in the three feeds for each 40 MHz segment of the full 300 MHz waterhole.

Figure 13 shows the signal path from the two sky beams. The most complex portion is the box labeled “80 megachannel FFT.” Happily, there has been considerable progress in both general purpose DSP (digital signal processor) ICs, and also in special purpose Fourier Transform ICs, either class of which could be used for this design. In order to cope with the flood of data emerging from the FFT ($400 \text{ megabytes s}^{-1}$ for this design) the design is highly parallel, with many identical paths

of smaller data bandwidth (based on the Serendip III architecture [Bowyer et al. 1992]) feeding an array of “backend” processors whose job is to monitor the spectra and keep track of the progress of recently identified spectral features. As with META, this new SETI spectrometer is intended for the detection of carriers and other spectrally narrow transmissions, and is insensitive to pulses and chirps.

We expect to use this new spectrometer system in a new set of continuous observations covering the waterhole. This SETI effort, which we call “Beta I” (Billion channel ExtraTerrestrial Assay), will carry out a high-resolution (0.5 Hz) full waterhole search of the northern sky, with its novel three-beam 0.24 gigachannel real-time digital spectrometer. With a follow-on system of 300 MHz instantaneous bandwidth, implemented as 6 gigachannels of 0.05 Hz resolution binwidth (“BETA II”), we intend to carry out a millihertz search of the waterhole. These projects represent an evolutionary approach to more powerful searches, in manageable steps that are achievable within the environment of university research.

In Table 3 we have drawn together the relevant parameters

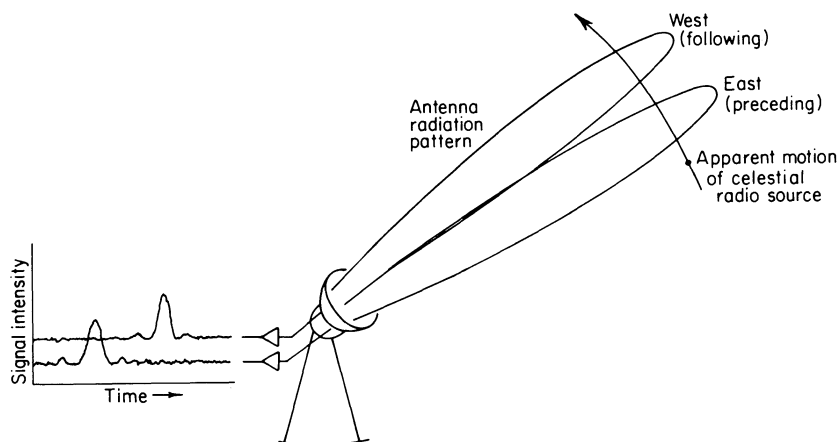


FIG. 12.—Dual-beam transit SETI. A third channel, fed from a low-gain all-sky horn, provides additional robustness against terrestrial sources.

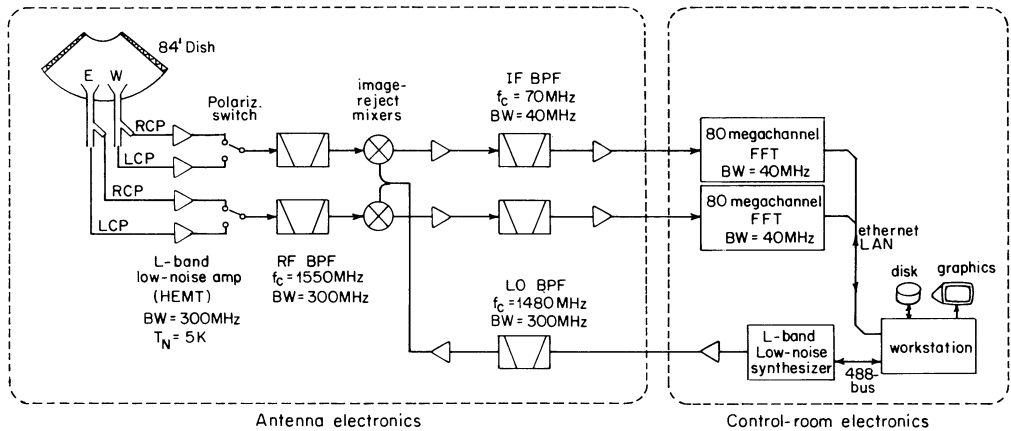


FIG. 13.—BETA I: Two sky beams plus a nondirectional terrestrial feed are simultaneously processed by 80 megachannel FFT spectrometers, in a wideband transit search. The spectrometer shares the architecture developed at Berkeley for the Serendip III search in progress at Arecibo.

of six contemporary and near-term search programs—META (Horowitz et al. 1986), Serendip III (Bowyer 1992), BETA I and II, and the NASA Sky Survey and Targeted Search (Tarter 1993)—along with Drake’s pioneering project Ozma (Drake 1960). The latter serves to highlight the impressive advances in channel count, bandwidth, and sky coverage that 3 decades of microchip technology have made possible. We compare these programs using Drake’s figure of merit, which probably does justice to none of the searches; it is a measure of the odds of success, assuming a homogeneous and isotropic distribution of civilizations transmitting weak signals at random frequencies. Briefly stated, Ozma was the world’s first serious search; META is the first megachannel search and the first ultrahigh spectral resolution search for carriers at preferred frequencies;

Serendip-III is the first megachannel high-sensitivity search at UHF; the NASA Sky Survey is the first all-sky search over the entire 10 GHz microwave window; the NASA Targeted Search is the first high-sensitivity, wideband search for carriers, pulses, and chirps (and their various combinations) from favorable nearby stars, covering the bottom 2 GHz portion of the microwave window; BETA I will be the first high-resolution dual-beam search, combining the all-sky coverage of the Sky Survey with the spectral resolution of the Targeted Search; and BETA II will be the first full-waterhole, ultrahigh resolution spectrometer, with true billion-channel capability. In their choice of sky coverage, resolution, and strategy, these evolving search programs are complementary, demonstrating a stunning growth in search capability over 4 decades.

TABLE 3
SELECTED SEARCHES

Parameter	OZMA	META	Serendip-III	BETA-I	BETA-II	NASA-SS	NASA-TS ^h	
							NAIC	NRAO
Number of channels (Mch)	0.000001	8.4	4	160	6000	32	15 ⁱ	
Resolution (Hz)	100	0.05	0.6	0.5	0.05	20	1,2,4,7,14,28,1k	
Instantaneous BW (MHz)	0.0001	0.4	2.4	40 ^c	300	320 ^f	10 ^{f,i}	
Total freq coverage (MHz)	0.36	1.2	12	320	300	9000	2000	
Sensitivity ^a (W/m ²)	6×10^{-22}	1.7×10^{-23j}	9×10^{-25}	4×10^{-23}	4×10^{-24}	$0.6-2 \times 10^{-22g}$	4×10^{-26}	5×10^{-25}
Total observing time ^b (khr)	0.2	44	8	44	44	35	3	44
Sky coverage (% of 4π)	0.0004%	70%	22%	70%	70%	100%	0.002%	0.1%
Types of signals ^c	C	C	C,CH,SC	C,SC	C	C,CH	C,CH,P	
RFI rejection	re-obs	anti-chirp	re-obs/dbase	dual-beam	anti-chirp	re-obs/dbase	re-obs/dbase	
Drake figure-of-merit ^d (GHz-m ³ /W ^{3/2})	1×10^{23}	1×10^{31j}	4×10^{33}	9×10^{32}	3×10^{34}	$0.4-2 \times 10^{34g}$	3×10^{35}	6×10^{33}

^a For SNR = 30: flux = $30 k_B T_{\text{sys}} B_{\text{ch}} / A_{\text{ant}} \eta_{\text{ant}} (B_{\text{ch}} \tau)^{1/2}$.
^b Over 5 years or project duration, whichever is less.
^c C = carrier; CH = chirp; P = pulse; SC = slow chirp.
^d DFM = (Total frequency coverage) × (Sky coverage)/Sensitivity^{3/2} (Drake 1983).
^e In each of two simultaneous beams.
^f In each of two simultaneous polarizations.
^g Sensitivity varies with frequency: $\tau(s) = 2.7/f(\text{GHz})$.
^h Portions of the NASA targeted search will be carried out at NAIC (Arecibo, 305 m) and at NRAO (Green Bank, 46 m).
ⁱ Per module.
^j Mean value, averaged over FFT scalloping loss and antenna beam profile (see text).

META was constructed through a gift by Steven Spielberg to The Planetary Society (TPS). We thank the members of TPS for their continuing and enlightened support over a decade, as well as the NASA Ames Research Center for support during construction of Suitcase SETI, from which the META project evolved. In addition to TPS support, BETA I is receiving funding from NASA and the Bosack/Kruger Charitable Foundation; its spectrometer core is based on the Serendip III architecture developed by Stu Bowyer's group at the University of California at Berkeley. We thank the Dudley Observatory and the Hofheinz Foundation for small supplementary grants. The first author is indebted to Michael Davis, Frank Drake, Philip Morrison, Edward Purcell, and the second

author, for continuing wisdom and encouragement over the years. We thank Guillermo Lemarchand and James Cordes for their most valuable suggestions and help; John Forster, Ivan Linscott, and Brian Matthews for essential contributions to META; Nancy Hecker for data reduction; Darren Leigh for calculation of ephemerides; Joe Caruso, Richard McCrosky, Skip Schwarz, and Robert Stefanik, who were the crucial support staff at the George Russel Agassiz Station site at Harvard, Massachusetts; and Stu Bowyer, Michael Davis, Bob Dixon, Frank Drake, Freeman Dyson, Lou Friedman, Ken Kellermann, John Kraus, Phil Morrison, Bruce Murray, Ed Purcell, Woody Sullivan, and Jill Tarter for critical comments on the manuscript.

REFERENCES

- Bowyer, S., Wertheimer, D., Donnelly, C., Lampton, M., Herrick, W., Soller, J., Ng, D., & Hiatt, T. 1992, *PASP*, in press
 Cocconi, G., & Morrison, P. 1959, *Nature*, 184, 844
 Cordes, J. M., & Lazio, T. J. 1991, *ApJ*, 376, 123
 ———. 1992, *PASP*, in press
 Davis, M. M. 1990, private communication
 Dixon, R., & Tarter, J. 1991, separate comments at The Planetary Society Conf., "SETI: Consequences of Non-Detection" (Cambridge, MA) (P. Morrison, moderator)
 Drake, F. D. 1960, *Sky and Telescope*, 19, 140
 ———. 1983, NASA Tech. Paper 2244
 Groth, E. J. 1975, *ApJS*, 29, 285
 Hart, M. 1975, *QJRAS*, 16, 128
 Heidmann, J., Biraud, F., & Tarter, J. 1989, Pulsar-Aided SETI Experimental Observations. IAA-89-642 (presented at the International Academy of Astronautics Meeting, Torremolinos, Spain)
 Hester, L. (Fujitsu Semiconductor Corp.), 1992, private communication
 Horowitz, P. 1987, *Planet. Rep.*, 7 (4), 8
 Horowitz, P., & Clubok, K. 1992, *Acta Astron.*, 26, 193
 Horowitz, P., Matthews, B. S., Forster, J., Linscott, I., Teague, C. C., Chen, K., & Backus, P. 1986, *Icarus*, 67, 525
 Kardashev, N. S. 1964, *Soviet Astron.*—*AJ*, 8, 217
 Morrison, P., Billingham, J., & Wolfe, J. 1977, *The Search for Extraterrestrial Intelligence*, NASA SP-419 (Washington, DC: US GPO)
 Oliver, B. M., & Billingham, J. 1972, *Project Cyclops: A Design Study of a System for Detecting Extraterrestrial Intelligent Life*, NASA CR-114445 (Washington, DC: US GPO)
 Sagan, C., ed. 1973, *Communication with Extraterrestrial Intelligence* (Cambridge, MA: MIT Press)
 Sagan, C., et al. 1982, *Science*, 218, 426
 Shklovskii, I. S., & Sagan, C. 1966, *Intelligent Life in the Universe* (New York: Dell)
 Tarter, J. C. 1991, *The Search for Life Beyond the Solar System* (presented at the Frontiers of Life Conf., Chateau de Blois, France)
 ———. 1993, *Summary of SETI Observing Programs* (Palo Alto, CA: SETI Institute; revised annually)
 Tipler, F. J. 1980, *QJRAS*, 21, 3, 267
 Yerazunis, W. (Digital Equipment Corp.) 1992, private communication